Proceedings of the European Conference "Physics of Magnetism" (PM'08), Poznań 2008

Activation Energies of Crystallization in Amorphous $RMn_{4.5}Ge_{4.5}Fe_{1.5}Al_{1.5}$ (R = La, Y, Dy) Alloys

Z. Śniadecki[a], U.K. Rössler[b] and B. Idzikowski[a]

[a]Institute of Molecular Physics, Polish Academy of Sciences
M. Smoluchowskiego 17, 60-179 Poznań, Poland

[b]IFW Dresden, P.O. Box 270116, D-01171 Dresden, Germany

The effective activation energies, characteristic crystallization temperatures and enthalpies of amorphous $RMn_{4.5}Ge_{4.5}Fe_{1.5}Al_{1.5}$ (R = Y, La, Dy) alloys produced using melt-spinning technique were investigated by differential scanning calorimetry. X-ray diffraction measurements were performed for as-quenched and annealed samples. The crystalline structure of annealed $YMn_{4.5}Ge_{4.5}Fe_{1.5}Al_{1.5}$ and $DyMn_{4.5}Ge_{4.5}Fe_{1.5}Al_{1.5}$ alloys was determined as orthorhombic $TbFe_6Sn_6$-type with *Cmcm* (63) space group. The alloy with Y appears as a more useful non-magnetic analogue for $DyMn_{4.5}Ge_{4.5}Fe_{1.5}Al_{1.5}$ than the La-based alloy. The differential scanning calorimetry curves for Dy- and Y-based alloys also exhibit similar thermal behavior. The effective activation energies E_a were determined using the Kissinger approach and high values up to 778 ± 74 kJ/mol for La-based sample were established. The comparison of Y-, La-, and Dy-based alloys suggests improvement of thermal stability with the increase in rare-earth element atomic radius in the glassy $RMn_{4.5}Ge_{4.5}Fe_{1.5}Al_{1.5}$ systems.

PACS numbers: 61.43.Dq, 61.82.Bg, 75.50.Kj, 81.70.Pg

1. Introduction

The multicomponent $RMn_{6-x}Ge_{6-x}Fe_xAl_x$ ($0 \leq x \leq 6$) system with R = La, Y, Dy is derived from ternary compounds combining transition metals (TM) Fe and Mn, rare-earths element (R), and a metalloid or other metal (M) Ge and Al. Some compositions of this series with Dy have already been obtained in fully amorphous state, and it was shown that they display interesting and complex magnetic properties [1–3]. Also for R = La and Y amorphization is attainable in the same range of compositions. The alloys containing La and Y atoms without magnetic moments provide useful analogues in order to understand the influence of the rare-earth magnetic moments on the magnetism in the alloys with Dy or with other rare earths. However, subtle changes in structure and stability could be induced by the different sizes of the R ions in the $RMn_{6-x}Ge_{6-x}Fe_xAl_x$ system. This is the main scope of this paper, which reports determination of changes in calorimetric data and structure with different rare-earth element substitution. We focus on the $RMn_{4.5}Ge_{4.5}Fe_{1.5}Al_{1.5}$ composition, which was described for R = Dy in more detail and was found to occupy the center of the glass-forming region in the composition series $DyMn_{6-x}Ge_{6-x}Fe_xAl_x$ [1]. In relation to the glass-forming ability (GFA), it is important that the structure and the stability of the ternary intermetallic compounds with limiting composition RMn_6Ge_6 and RFe_6Al_6 depend on the ion radius of the lanthanide or rare-earth atoms.

The $DyMn_{6-x}Ge_{6-x}Fe_xAl_x$ ($0 \leq x \leq 6$) alloy series is based on the two parent compounds $DyFe_6Al_6$ and $DyMn_6Ge_6$. $DyMn_6Ge_6$ crystallizes in the hexagonal $HfGe_6Fe_6$-type structure ($P6/mmm$) [4, 5]. Full substitution of Mn and Ge by Fe and Al leads to the creation of the second parent compound. $DyFe_6Al_6$ has a disordered $CeMn_4Al_8$-type structure with $I4/mmm$ space group [4]. However, the $RMn_{6-x}Ge_6$ with light rare earths or La crystallize in the YCo_6Ge_6 structure belonging to the hexagonal $P6/mmm$ space group [4, 6, 7]. On the other hand, the tetragonal compounds RFe_6Al_6 only form for the heavy rare earths, for Y and U and do not form for La and the light rare earths [8].

Here we report results obtained with X-ray diffraction (XRD) and differential scanning calorimetry (DSC). The crystallization process in $RMn_{4.5}Ge_{4.5}Fe_{1.5}Al_{1.5}$ (R = La, Y, Dy) samples was analyzed. In particular, characteristic temperatures, enthalpies and effective activation energies were determined. These data indicate good GFA and stability of these materials. In general, these parameters are useful in planning of annealing routes and in determining optimum compositions for new nanostructured materials with properties that can be controlled by adjusting different structural states, especially different grain sizes of nanocrystalline or mixed crystalline-amorphous materials. Samples were also annealed, mainly to define crystalline structures.

2. Experiment

The prealloys were prepared by arc melting of high purity elements. With the use of melt-spinner apparatus with copper wheel, ribbons with thickness of 50–70 μm

were spun. The preparation process was done in protective atmosphere (Ar) to avoid oxidation. Structural information was obtained by XRD either using a Philips X'Pert or a HZG-4 diffractometer both with Co K_α radiation in the Bragg–Brentano geometry. The crystallization process of as-quenched samples was investigated by DSC measurements using Netzsch DSC 404 equipment between room temperature and 900°C with different heating rates $10 \leq q \leq 50$ K/min. Heat treatment was carried out in a standard furnace in isothermal mode.

3. Results and discussion

A fully amorphous state (Fig. 1) was obtained for $LaMn_{4.5}Ge_{4.5}Fe_{1.5}Al_{1.5}$ and $YMn_{4.5}Ge_{4.5}Fe_{1.5}Al_{1.5}$ alloys due to the same physical reasons as reported earlier for $DyMn_{4.5}Ge_{4.5}Fe_{1.5}Al_{1.5}$ [1]. There is a competition between amorphous state formation and crystallization of ternary parent compounds. The main forces leading to destabilization of the crystalline structure and simultaneously to stabilization of the amorphous state are frustrated repulsive chemical interactions between some of the alloy constituents [1].

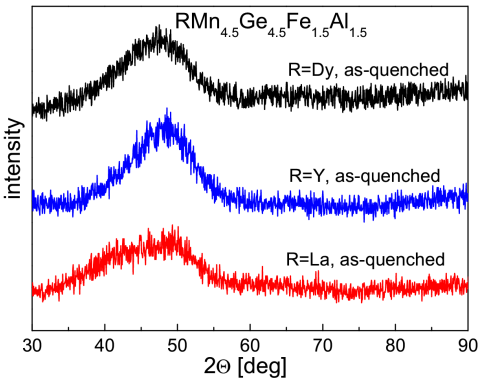

Fig. 1. X-ray diffraction patterns for as-quenched $RMn_{4.5}Ge_{4.5}Fe_{1.5}Al_{1.5}$ (R = Dy [1], Y, La) amorphous alloys.

Two exothermic peaks are observed on heat flow curves for $DyMn_{4.5}Ge_{4.5}Fe_{1.5}Al_{1.5}$ and $YMn_{4.5}Ge_{4.5}Fe_{1.5}Al_{1.5}$ samples (Fig. 2). First peak is very distinct while the second one which appears slightly below 700°C is less apparent and wider on the temperature scale. $LaMn_{4.5}Ge_{4.5}Fe_{1.5}Al_{1.5}$ has more complex and significantly different characteristic as those observed for Dy and Y containing alloys. It also undergoes crystallization in two steps. A deconvolution of the first peak (inset of Fig. 2) reveals two crystallization steps, where the second step starts and proceeds very rapidly during the first slower process. This situation is contrary to typical two-step crystallization processes as, e.g., often observed for Fe-based metallic glasses [9] and also for the alloys with 1:6:6 stoichiometry, containing Dy and Y, where the second step is sluggish and typically connected with grain growth. Deconvolution of the first

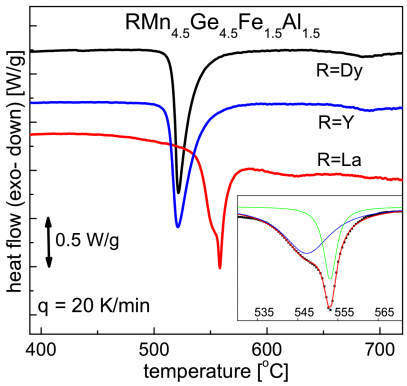

Fig. 2. DSC curves for as-quenched $RMn_{4.5}Ge_{4.5}Fe_{1.5}Al_{1.5}$ (R = Dy [1], Y, La) amorphous alloys. Inset shows the deconvolution of the first exothermic peak for $LaMn_{4.5}Ge_{4.5}Fe_{1.5}Al_{1.5}$ sample.

peak provides information about the contribution of both processes to the transformation heat (first process — 71%, second process — 29%) and this contribution varies slightly without any clear trend for different heating rates. DSC measurements were made in isochronal (dynamic) mode at different heating rates varied from 10 to 50 K/min. Crystallization temperature (peak maximum) T_p and the enthalpies ΔH of the crystallization processes were determined. The crystallization effects observed on DSC curves, depend on time and temperature. Therefore, at higher heating rates, due to the more delayed sample response, the reaction starts at higher temperatures and the crystallization peak is shifted. Crystallization temperatures vary from 514°C to about 529°C for $YMn_{4.5}Ge_{4.5}Fe_{1.5}Al_{1.5}$ and from 553°C to 564°C for $LaMn_{4.5}Ge_{4.5}Fe_{1.5}Al_{1.5}$. In comparison with Dy containing alloys ($516°\mathrm{C} \leq T_\mathrm{p} \leq 532°\mathrm{C}$) there is only a slight decrease for $YMn_{4.5}Ge_{4.5}Fe_{1.5}Al_{1.5}$ sample. This fact and the similar character of the crystallization process suggest that in these two alloys the devitrification creates crystalline compounds with the same structure. This was confirmed from the XRD patterns of these alloys isothermally annealed just below crystallization temperatures for 15 min (Fig. 3). The enthalpies of the first (dominant) crystallization event were also determined. Their values are $\Delta H = 78$ J/g and 55 J/g for $YMn_{4.5}Ge_{4.5}Fe_{1.5}Al_{1.5}$ and $LaMn_{4.5}Ge_{4.5}Fe_{1.5}Al_{1.5}$, respectively. The value for the Y containing alloy is similar to the crystallization enthalpy value of $\Delta H = 73$ J/g obtained for Dy containing alloy. All enthalpies were determined from measurements at $q = 20$ K/min, but the heating rate did not significantly influence the determined values of ΔH. No signs of glass transition were observed for La- and Y-based amorphous alloys in the DSC scans. This behavior is similar to that reported earlier for $DyMn_{6-x}Ge_{6-x}Fe_xAl_x$ [1, 3]. There are different suggested explanations for this absence of a clear signature for the glass transition [1]. The amorphous structure could be composed from different polyamorphous states with a wide range of local glass

transitions or the glass transition temperatures could be close or above crystallization temperature. Therefore, this effect would be hidden by the more apparent crystallization process.

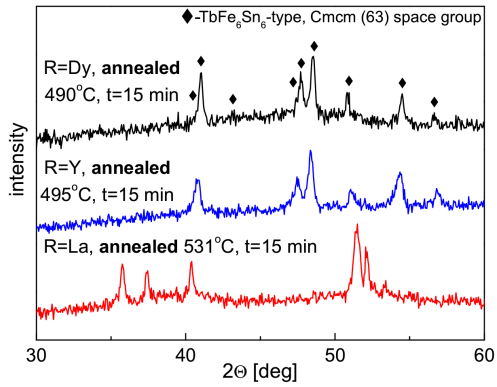

Fig. 3. XRD patterns of $RMn_{4.5}Ge_{4.5}Fe_{1.5}Al_{1.5}$ (R = Dy [1], Y, La) alloys isothermally annealed for 15 min at temperatures just below T_p.

As-quenched samples were annealed at temperatures just below the first crystallization peak to obtain partially crystalline and single phase alloys. $DyMn_{4.5}Ge_{4.5}Fe_{1.5}Al_{1.5}$ (Fig. 3) crystallizes in orthorhombic $TbFe_6Sn_6$-type structure with *Cmcm* (number 63) space group as already found earlier [4]. Also amorphous $YMn_{4.5}Ge_{4.5}Fe_{1.5}Al_{1.5}$ alloy crystallizes in the same structure. On the other hand, the devitrification of the La based alloy leads to the formation of different crystalline structures, which could not be identified yet. This difference in the crystallization products between the alloys with Dy or Y and with La was already suggested by the different character of the crystallization process of these alloys, seen from the DSC analysis. Effective activation energies E_a of the first crystallization event were calculated using the Kissinger method (slope of the Kissinger plot) [10]. Both, T_p and T_o (onset of crystallization) temperatures were used to determine the E_a values (Figs. 4 and 5). The Kissinger analysis based either on T_p or on T_o yields slightly different parameters. For the two alloys with Y and La, E_a values calculated from T_p and T_o temperatures are different. This is due to the fact that T_p shifts to higher temperatures relative to the onset temperatures T_o, which is connected with the broadening of DSC peaks with increasing heating rate. The analysis using T_p probably gives the better estimate of the activation energy, and the additional set of parameters can serve to quantify their uncertainty. Hence, the activation energy from the fits is $E_a = 577 \pm 87$ kJ/mol for $YMn_{4.5}Ge_{4.5}Fe_{1.5}Al_{1.5}$, while for $LaMn_{4.5}Ge_{4.5}Fe_{1.5}Al_{1.5}$ it increases up to 778 ± 74 kJ/mol.

These values exceed the activation energy determined earlier for $DyMn_{4.5}Ge_{4.5}Fe_{1.5}Al_{1.5}$ [3] which reaches only 455 ± 40 kJ/mol. These rather large changes in E_a could be due to the different atomic radii of these rare earths with Dy having the smallest atomic radius $r = 0.1774$ nm, while Y has a radius $r = 0.18015$ nm. The La atoms still have a bigger radius $r = 0.1879$ nm and, as expected, for La-based alloy E_a reaches an even larger value.

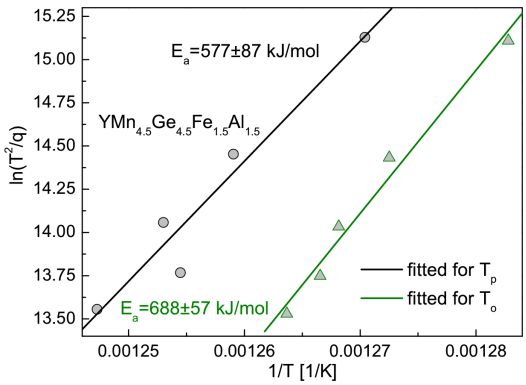

Fig. 4. Kissinger plot for the first crystallization effect for melt-spun $YMn_{4.5}Ge_{4.5}Fe_{1.5}Al_{1.5}$ ribbon (circles and triangles are calculated from T_p and T_o, respectively).

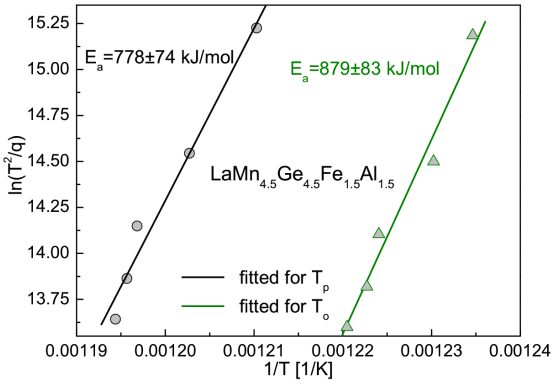

Fig. 5. Kissinger plot for the first crystallization effect for the melt-spun $LaMn_{4.5}Ge_{4.5}Fe_{1.5}Al_{1.5}$ ribbon (circles and triangles are calculated from T_p and T_o, respectively).

The amorphous structure in this group of alloys is an example of 7 at.% solute with a large radius (rare-earth elements) dissolved in an amorphous matrix of smaller atoms (Mn, Ge, Al, Fe) with rather similar sizes but different and partially repulsive pairwise chemical interactions. We have found a clear trend of increasing E_a with increasing radius r of the solute. This trend can be understood from the theory of atomic-level stresses proposed by Egami and Waseda [11, 12], which emphasizes the importance of large radii-differences between solute and solvent for GFA and for the stability of multinary amorphous packings.

4. Summary

Samples of $LaMn_{4.5}Ge_{4.5}Fe_{1.5}Al_{1.5}$ and $YMn_{4.5}Ge_{4.5}Fe_{1.5}Al_{1.5}$ were successfully prepared in fully amorphous state. This ascertains the high GFA

in this class of multinary alloys also for other rare earths than the previously investigated Dy-based systems [1]. Thermal characteristics (DSC) and crystalline structures of annealed samples of $YMn_{4.5}Ge_{4.5}Fe_{1.5}Al_{1.5}$ are similar to the properties of the $DyMn_{4.5}Ge_{4.5}Fe_{1.5}Al_{1.5}$ alloy [3]. However, the crystallization process and its products are different for $LaMn_{4.5}Ge_{4.5}Fe_{1.5}Al_{1.5}$, which indicates the importance of the R-radius in this alloys system. As $YMn_{4.5}Ge_{4.5}Fe_{1.5}Al_{1.5}$ and $DyMn_{4.5}Ge_{4.5}Fe_{1.5}Al_{1.5}$ show only very small differences in structure and thermal properties, the Y-based alloy could be used to separate the magnetic contribution of R atoms in heat capacity or resistivity measurements. These two alloys may allow one to disentangle the relevance for the magnetic properties of the amorphous mixed FeMn-subsystem and of the rare earth $4f$ electron-magnetism due to Dy. It remains to be proved, whether amorphous or nanocrystalline alloys in this system can also be produced with early rare-earth atoms, as Nd or Pr, with atomic radii in between the larger radius of La and the smaller radii of Dy and Y. Very high values of effective activation energies, especially for La-based alloy, were determined. This suggests the high thermal stability of all investigated systems. The amorphous state stability is connected with high glass forming ability. This fact suggests the possibility of bulk metallic glasses fabrication in this multinary alloy system.

Acknowledgments

This work was supported by the funds for science in years 2007–2009 as a research project No. N202 088 32/2030. Authors appreciate financial support from Project Based Personal Exchange Programme with DAAD/MNiSW in years 2007–2008.

References

[1] P. Kerschl, U.K. Rößler, T. Gemming, K.-H. Müller, Z. Śniadecki, B. Idzikowski, *Appl. Phys. Lett.* **90**, 031903 (2007).

[2] Z. Śniadecki, B. Idzikowski, J.-M. Greneche, P. Kerschl, U.K. Rößler, L. Schultz, *J. Phys., Condens. Matter* **20**, 425212 (2008).

[3] Z. Śniadecki, B. Idzikowski, *J. Non-Cryst. Solids* **354**, 5159 (2008).

[4] G. Venturini, R. Welter, B. Malaman, *J. Alloys Comp.* **185**, 99 (1992).

[5] P. Schobinger-Papamantellos, F.B. Altorfer, J.H.V.J. Brabers, F.R. de Boer, K.H.J. Buschow, *J. Alloys Comp.* **203**, 243 (1994).

[6] E. Parthé, B. Chabot, in: *Handbook on the Physics and Chemistry of Rare Earths*, Eds. K.A. Gschneidner, J.L. Eyring, Vol. 6, Elsevier Science, 1996, p. 113.

[7] P. Schobinger-Papamantellos, G. André, J. Rodríguez-Carvajal, N.P. Duong, K.H.J. Buschow, *J. Magn. Magn. Mater.* **231**, 121 (2001).

[8] W. Suski, in: *Handbook on the Physics and Chemistry of Rare Earths*, Eds. K.A. Gschneidner, J.L. Eyring, Vol. 22, Elsevier Science, 1996, p. 143.

[9] S. Kostyrya, Z. Śniadecki, B. Idzikowski, *Phys. Status Solidi B* **242**, 621 (2005).

[10] H.E. Kissinger, *Anal. Chem.* **29**, 1702 (1957).

[11] T. Egami, *J. Non-Cryst. Solids* **205-207**, 575 (1996).

[12] T. Egami, Y. Waseda, *J. Non-Cryst. Solids* **64**, 113 (1984).